Leakage-induced and disorder-activated modes from the folded acoustic branches in GaAs-AlAs superlattices

J. Sapriel, J. Chavignon, F. Alexandre, and R. Azoulay
Centre National d'Etudes des Télécommunications, 196 avenue Henri Ravera, 92220 Bagneux, France
(Received 16 May 1986)

Low-frequency Raman modes in the acoustic region (5–40 cm^{-1}) are investigated in (001)-oriented GaAs-AlAs superlattices grown by molecular-beam epitaxy and metal-organic chemical-vapor deposition. Besides the well-known folded LA (FLA) modes, we carefully studied the folded TA (FTA) modes and also modes corresponding to the zone edge of the folded acoustic (LA and TA) branches. The former modes fulfill the selection rule of wave-vector conservation and are due to a leakage of the light polarization. The latter are activated by the disorder and are influenced by the interface defects. These disorder-activated (DA) modes, called DAFLA and DAFTA, are propagative modes which are sensitive to the period of the superlattice, contrary to the previously reported DALA and DATA which are localized in the GaAs and AlAs layers and whose frequency is fixed.

I. INTRODUCTION

So far Raman scattering studies on GaAs-AlAs superlattices in the acoustic range were focused on modes belonging to the folded longitudinal acoustic (LA) branch.[1,2] In the case of acoustic propagation along the z axis (perpendicular to the layers), such modes are Raman active of symmetry A_1 and their intensity is about ten times smaller than the intensity of the LO in GaAs and AlAs. In this paper we investigate new Raman lines whose intensity is only a few percent of that of the folded LA modes and whose frequency is much lower. Their observation is consequently more difficult because of the spurious elastically scattered light. These drawbacks are overcome only by using a very sensitive experimental setup with high stray-light rejection.

The first kind of modes reported here are folded transverse acoustic (TA) modes. They are normally forbidden for a propagation along the z axis, but are observed because of a "leakage" due to Brewster incidence and to the aperture of the scattered light collecting lens. These two effects add to create a small polarization component of the light along z, thus inducing a Raman activity.[2] As with the folded LA, the folded TA modes, which fulfill the selection rule of wave-vector conservation common to all scattering processes, appear as doublets of two lines of comparable intensity. Besides, they can be clearly observed for all scattering polarizations.

The other kind of investigated modes give Raman structures of symmetry A_1 [spectra (x,x) or (y,y)] at frequencies lower than the folded LA and TA. Two distinct peaks generally appear, corresponding to the lowest energy Brillouin-zone edges in the z direction. One of the peaks is related to the folded LA branch, and the other to the folded TA branch. These modes correspond to the first maximum of the phonon density of states in the folded Brillouin zone. They are not allowed by the Raman selection rules, but a small amount of disorder can activate them. We shall thus call them DAFTA (disorder-activated folded transverse-acoustic modes) and DAFLA (disorder-activated folded longitudinal-acoustic modes) to differentiate them from the well-known DATA and DALA of zinc-blende binary crystals[3] and ternary alloys.[4] Contrary to DATA and DALA, which correspond to the zone edge π/a of the Brillouin zone (and are thus located at much more higher fixed frequencies), DAFTA and DALTA have a strong frequency dependence on the superlattice period D.

II. THEORETICAL BACKGROUND

The frequency Ω_p of the folded acoustic modes involved in the backscattering process along z in a superlattice of the same type as GaAs-AlAs is given[2] by the approximate relation

$$\Omega_p = 2\pi V \left[(-1)^p \frac{2n}{\lambda} + \frac{1}{D} \left\lfloor \frac{p+1}{2} \right\rfloor \right] . \tag{1}$$

Here p is the folding order, λ is the wavelength of light in vacuum, n and V are the refractive index and the acoustic velocity in the superlattice, D is the period ($D=d+d'$), $\lfloor (p+1)/2 \rfloor$ is the integral part of $(p+1)/2$, and V can be expressed as a function of the thickness d and d', acoustic velocities v and v', and densities ρ and ρ' of the constituent layers:

$$V = D \left[\frac{d^2}{v^2} + \frac{d'^2}{v'^2} + \frac{dd'}{vv'} \left[Z + \frac{1}{Z} \right] \right]^{-1/2} . \tag{2}$$

Here $Z=\rho v/\rho' v'$ is the ratio of the acoustic impedances.

Equations (1) and (2) are valid for longitudinal (elastic constants C_{33} and C'_{33}) as well for transverse modes (C_{44} and C'_{44}). In Eq. (1), the gaps between the folded acoustic branches are neglected. This situation is characteristic of GaAs-AlAs superlattices where Z is not very different from 1.

If V_L and V_T are the longitudinal- and transverse-acoustic wave velocity in the superlattice,

$$\frac{V_L}{V_T}=\left[\frac{C_{33}^{\text{eff}}}{C_{44}^{\text{eff}}}\right]^{1/2}. \quad (3)$$

C_{44}^{eff} and C_{33}^{eff} are effective elastic constants in the superlattice and are given by[5]

$$(C_{44}^{\text{eff}})^{-1}=(dC_{44}^{-1}+d'C'^{-1}_{44})/D\ , \quad (4)$$

$$(C_{33}^{\text{eff}})^{-1}=(dC_{33}^{-1}+d'C'^{-1}_{33})/D\ . \quad (5)$$

The determination of V_L (V_T) is directly obtained from the frequencies Ω_1 and Ω_2 of the first folded longitudinal (transverse) doublet according to V_L (V_T)$=(\Omega_1+\Omega_2)D/4\pi$. The lowest frequency of the Brillouin-zone edge (BZE) along z is given by $(\Omega_1+\Omega_2)/4$. This frequency corresponds approximately to the center of the first gap at $k=\pi/D$ in the case where its magnitude is no more neglected. One can distinguish between $(\text{BZE})_L$ and $(\text{BZE})_T$ according to the doublet Ω_1,Ω_2 under consideration (longitudinal$_L$ or transverse$_T$).

III. EXPERIMENTAL RESULTS

The set of experiments reported and discussed here is self-consistent. More precisely, the measurements of the components of the folded TA and LA doublets allow the determination of the Brillouin-zone-edge frequencies $(\text{BZE})_T$ and $(\text{BZE})_L$. These frequencies, in turn, are compared to those of the DAFTA and DAFLA in the low-frequency part of the Raman spectra to confirm their assignment.

We used a Ramanor U 1000 double monochromator from Jobin-Yvon in the photon-counting mode. The experiments were performed at room temperature and liquid-nitrogen temperature with the 5145-, 4880-, and 4765-Å chief lines of an argon-ion laser. The photomultiplier dark current was about a few counts/sec and the monochromator scanning was 0.1 cm^{-1}/min in order to extract the Raman signal from the noise.

A series (A) of molecular-beam epitaxy (MBE)-grown GaAs-AlAs superlattice of period $\simeq$40 Å, obtained with different experimental conditions of growth, were investigated. A quantitative estimation of the interface width d_0 of these samples has been obtained from the intensity of the folded LA modes and from the frequency of the optical phonons confined in GaAs layers (see Ref. 6 for the definition and the estimate of d_0).

Besides, a GaAs-AlAs superlattice (sample B) prepared by metal-organic chemical-vapor deposition (MOCVD) with a period of $\simeq$80 Å as well as a 48-Å period GaAs-$Ga_{0.7}Al_{0.3}As$ superlattice, grown by MBE (sample C), were both studied for comparison.

A. The folded TA modes

In Fig. 1 we report the spectrum obtained for sample B. Eight prominent modes (labeled for 1 to 8) are observed, which correspond to the folded LA. In addition, one can see new small modes (indicated by arrows). For crossed incident and scattered polarizations, the intensity of all the Raman lines cancels except the two doublets of Figs. 2(a) and 2(b), which correspond to the first, second, third, and fourth folded TA. In Fig. 2(c) one can see the first and second folded TA modes at room temperature and at 80 K obtained on a sample of the series A. All these lines are very sharp (on the order of 1 cm^{-1} or less). The two components of the doublets are separated by $\Delta\omega=8\pi nV/\lambda$, i.e., the two lines are closer ($\sim$3.2 cm^{-1}) in the case of folded TA, than in the case of folded LA ($\sim$5 cm^{-1}).

In Table I are reported the frequencies of the first LA and TA doublets as a function of the sample of the series A. The ratio V_L/V_T is obtained with a good precision by dividing the two sums $(\Omega_1+\Omega_2)$ of the components of the folded LA and TA doublets. While V_L and V_T vary

TABLE I. Raman scattering investigation ($\lambda=5145$ Å) of the low-frequency (12–50 cm^{-1}) part of the acoustic region in the samples of series A. A_1 and A_6 are characterized by sharp interfaces, a small Si doping being present in GaAs layers of A_1; A_7 has broader interfaces; A_2 to A_5 are classified in order of increasing interface width d_0 according to Ref. 6. The labels a,b,c allow the distinction (due to inhomogeneity) between different points along the surface of the same sample. The ratio V_L/V_T of the longitudinal- and transverse-acoustic velocity in the superlattice is simply deduced from the measurement of the components of the folded LA and TA doublets (see text). V_L/V_T remains constant though the doublet frequencies undergo 20% variations. The measured values of DAFLA and DAFTA peaks are very close to the values $(\text{BZE})_L$ and $(\text{BZE})_T$ calculated from the experimental determination reported in columns 2 and 3.

SL Sample	Components of the first folded LA doublet (cm^{-1})	Components of the first folded TA doublet (cm^{-1})	V_L/V_T	$(\text{BZE})_L$ (cm^{-1})	DAFLA (cm^{-1})	$(\text{BZE})_T$ (cm^{-1})	DAFTA (cm^{-1})
$A\,1a$	39.55, 44.55	27.3, 30.3	1.46	21	19.8	14.4	14.05
$A\,1b$	37.75, 42.75	26., 29.25	1.46	20.1	19.25	13.9	14
A_2	40.55, 46.55	27.8, 31.05	1.46	21.5	20.55	14.7	15.5
A_3	38.55, 43.55	26.3, 29.8	1.46	20.5	19.6	14	14
A_4	39.05, 43.8	26.8, 30.05	1.46	20.7	19.8	14.2	14.3
A_5	41.0, 46	28.25, 31.5	1.46	21.75	21	14.9	14.75
A_6	40.5, 45.75	28, 31.2	1.46	21.6	21.5	14.8	16
$A\,7a$	45.65, 50.4	31.15, 34.15	1.47	24	25	16.3	16
$A\,7b$	44.4, 49.4	30.9, 33.9	1.45	23.45	24.5	16.2	16
$A\,7c$	44, 48.9	30.2, 33.1	1.46	23.3	22.5	15.8	16

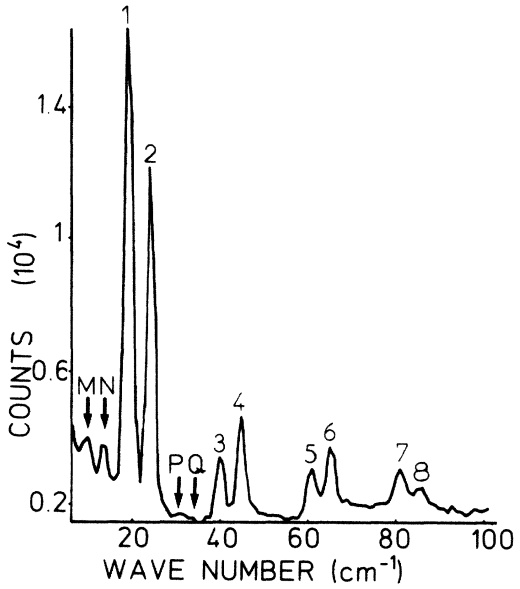

FIG. 1. A_1 spectrum of sample B in the acoustic region. The folded LA modes are labeled 1–8. Small intensity modes appear in addition and are indicated by arrows. Our study focused on these small lines; M is the disorder activated modes of Fig. 3(d). N is the first component of the first folded TA (the second one is not resolved in A_1 because of the proximity of the first folded (LA). P and Q are the two components of the second folded TA. To clearly extract the first and second TA doubled we used the x,y configuration for sample B [see Figs. 2(a) and 2(b)] which extinquishes the FLA.

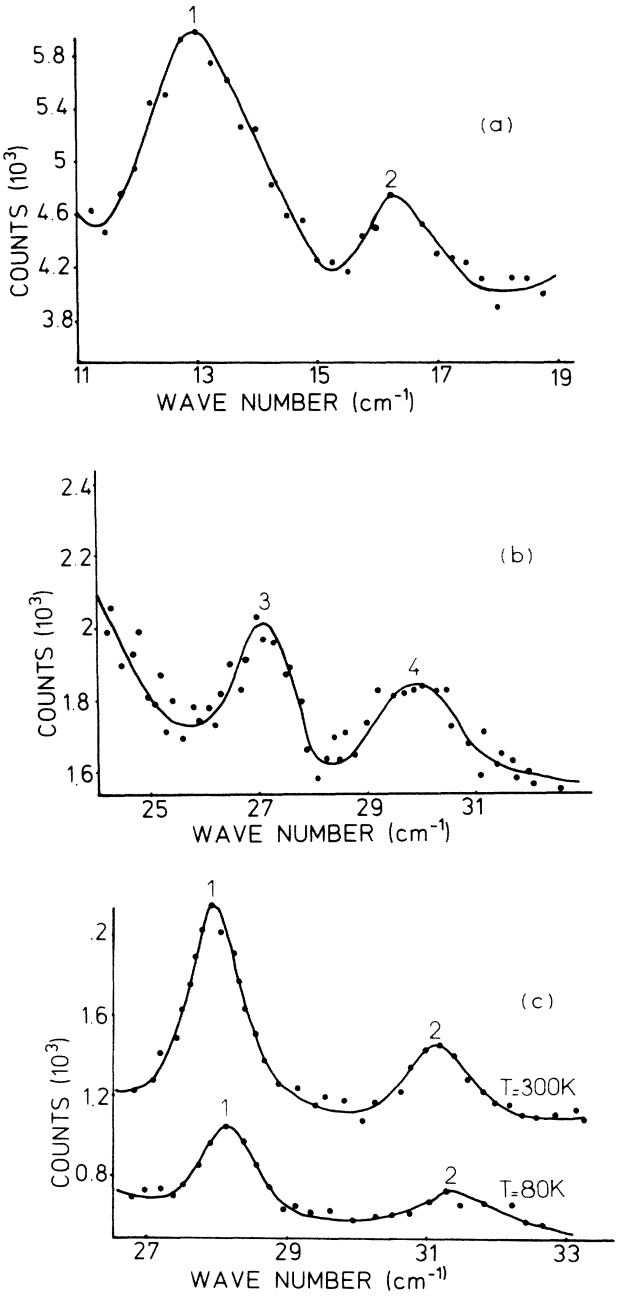

FIG. 2. Folded TA modes (a) First doublet (sample B). (b) Second doublet (sample B). (c) First doublet at 300 and 80 K in A_6 (the sharpest-interface sample of series A).

from sample to sample, or, due to inhomogeneities, from point to point along the surface of the same sample, their ratio remains constant and equal to 1.46 ± 0.01. From Eqs. (3), (4), and (5) it is clear that for $C_{33}=C'_{33}$ and $C_{44}=C'_{44}$, the ratio V_L/V_T is insensitive to variations of period and relative layer thicknesses in the superlattice. This is consistent with the assumption, supported by the similarities of the structural properties (same zinc-blende structure, same lattice parameter) that the elastic constants C_{33} and C_{44} undergo only very small variations in the $Ga_{1-x}Al_xAs$ system.[2] Thus, the replacement of Ga by Al is regarded as a mass change only. Actually, V_L/V_T is in good accordance with the ratio C_{33}/C_{44} in GaAs, given in the literature. Let us point out that folded TA as well as folded LA fulfill the wave-vector conservation conditions in the scattering process of the incident photon by the phonon contrary to the modes which are studied in the next section.

B. Disorder-activated folded acoustic modes

The DAFTA and DAFLA are the lowest frequency phonon modes ever observed in superlattices. They correspond to the zone edge ($K_z=\pi/D$) of the folded Brillouin zone where the density of the phonon states undergoes a maximum, due to the curvature of the phonon branches in the vicinity of the Brillouin-zone boundaries. Only the modes corresponding to the lowest-energy branches in the vicinity of π/D are seen because they are favored by the Bose statistics.

The DAFTA and DAFLA in GaAs-AlAs superlattices are represented in Fig. 3. As the DATA and DALA, they appear only in A_1 spectra. The energy of the Brillouin-zone edge is indicated by $(BZE)_T$ and $(BZE)_L$ for the transverse- and longitudinal-acoustic waves, respectively. One can notice the rather good agreement between the calculated values of $(BZE)_T$ and $(BZE)_L$, and the position of the DAFTA and DAFLA band peaks.

The width of these bands ($\sim$ a few cm^{-1}) is very small with respect to the width of the observed DATA and

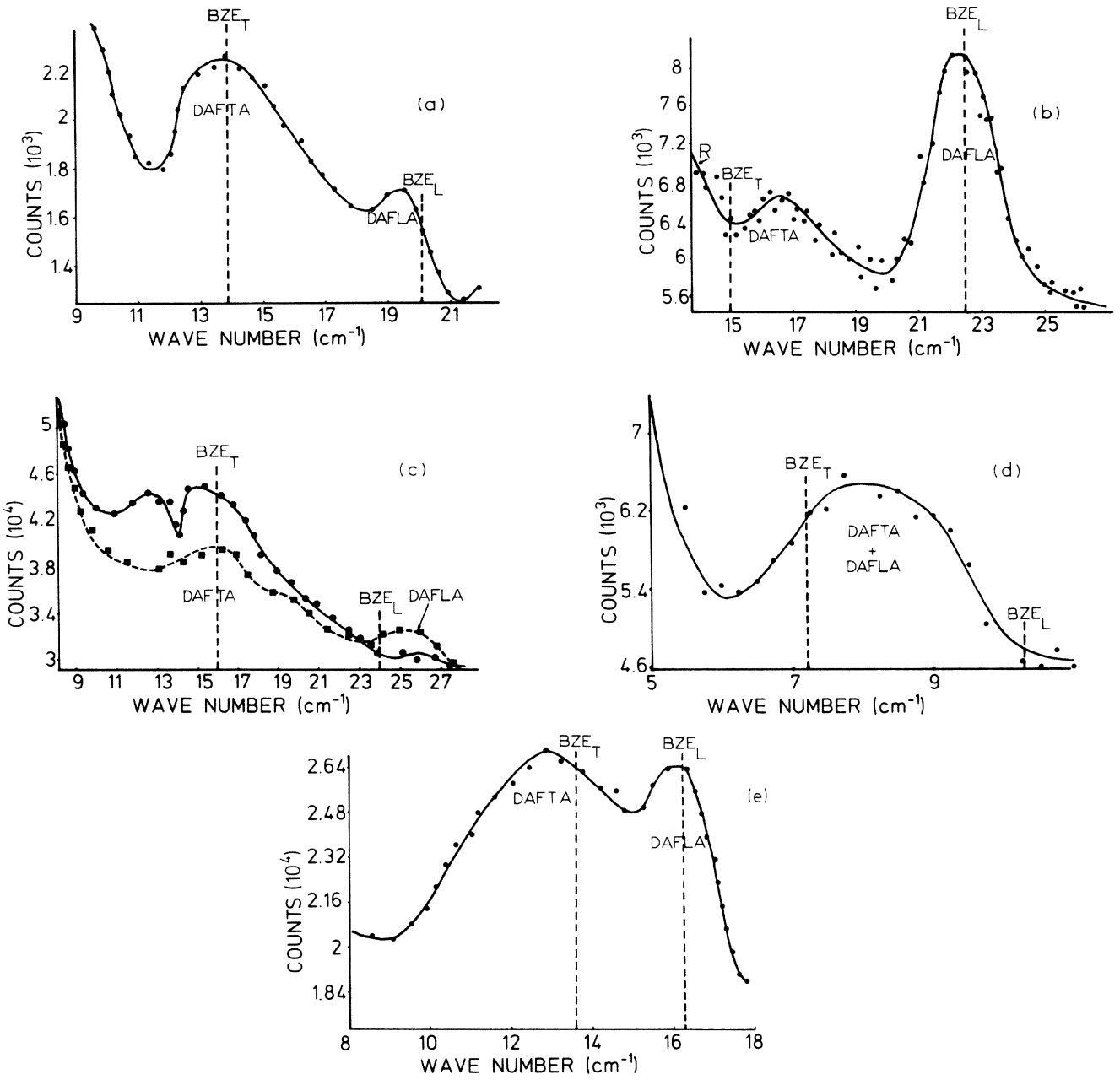

FIG. 3. DAFTA and DAFLA in samples A_1 (a), A_6, (b), A_7 in two different points of the surface solid and dashed lines of (c) and in sample B (d) whose period is about two times that of the series A. In sample B the DAFTA and DAFLA are too close to be resolved and merge into a single band. $(BZE)_T$ and $(BZE)_L$ are the lowest frequencies of the Brillouin-zone edge corresponding to folded TA and LA, respectively. The best-defined DAFTA and DAFLA correspond generally to the sharpest interface samples. A_1 and A_6 are characterized by sharp interfaces (d_0 less than 1.5 Å), A_7 by broad interfaces ($d_0 \simeq 5.3$ Å). The result of Raman investigation on sample C is reported in (e) (GaAs-$Ga_{0.7}Al_{0.3}As$ interfaces, period 48 Å).

DALA in GaAs, AlAs, and GaAs-AlAs superlattices.[2,7] Besides, the DAFTA is clearly larger than the DAFLA. This is due to the phonon density of states which is related to the dispersion of the phonon branches. A parallel can be drawn with the TA branches in GaAs and AlAs, which become flat for values of the wave vector k located between $\pi/2a$ and π/a in the Brillouin zone, though the LA branch is linear along nearly all the range of k values and flattens only in the vicinity of the Brillouin-zone edge.[8] The A_1 spectrum corresponding to another sample of the series characterized by sharp interfaces [Fig. 3(b)] shows that the DAFTA intensity is very low compared to that of the DAFLA in this case. Figure 3(c) corresponds to a sample with larger interfaces. The DAFTA increases markedly with respect to the DAFLA. This sample is inhomogeneous along the surface, and the spectra corresponding to two different points on the same sample exhibit noticeable differences although the general features

are qualitatively the same. The frequency of the DAFTA and DAFLA varies as the Brillouin-zone edge in the superlattices; i.e., as the inverse of the period D. For sample B ($D=82.5$ Å) the disorder-activated folded acoustic bands are observed at lower energies, but are too close to be resolved. The resulting band, which is seen on Fig. 3(d), clearly contains a main contribution from the DAFTA. The spectrum of Fig. 3(e) corresponds to sample C, which is a binary-ternary superlattice. Apart from the frequency reduction due to the change in the period, there is no difference with respect to the GaAs-AlAs superlattice of Fig. 3(a).

A question of interest is the origin of the disorder, which activates the modes which are issued from the Brillouin-zone edge. Contrary to DALA and DATA, which are localized in the constitutive layers of the superlattice and are a "signature" of GaAs and AlAs, DAFTA and DAFLA modes are propagative modes characteristic of the periodic structure and are actually a superlattice effect. It is likely that the interface defects somehow contribute to the formation of these bands. All the results obtained on the series A are reported in Table I. The positions of the observed DAFLA and DAFTA are indicated in columns 6 and 8 and are compared to the values of $(BZE)_L$ and $(BZE)_T$ calculated (see Sec. II) from the frequency measurements of the components of the first folded LA and TA doublets.

It is worthwhile to point out that the use of shorter photon wavelength increases the DAFTA intensity with respect to the DAFLA. This is probably due to the greater sensitivity of the DAFTA to surface defects, whose contribution is more important for smaller penetration depth of the light. The same DAFTA intensity enhancement with respect to the DAFLA is observed when the interfaces of the superlattice become broader.

In conclusion, we can say that these new structures, since they have been observed in both MBE and MOCVD, seem to be intrinsically related to the superlattice formation. All of the investigated superlattices in this paper are regularly periodic structures, and as checked by x rays and Raman scattering studies, have evidenced many folded acoustic modes as well "quantized" optic modes.[9] Thus the disorder can be considered as too small to really affect the periodicity. A stronger disorder would enhance the DALA and DATA to the detriment of the DAFLA and DAFTA. Though the DATA and DALA are localized in the individual layers and their spatial extension is a few periods a ($a \simeq 2.83$ Å in GaAs), the DAFTA and DAFLA propagate over several consecutive layers, otherwise they would not "see" the period D of the superlattice. In these conditions, it is likely that their behavior is influenced by the encountered interfaces.

We have reported the chief features of the DAFTA and DAFLA, but conclusions on the interfaces microscopic structure are to be expected from subtle variations of the Raman spectra. As these modes are at very low frequency, a detailed study of the profile is difficult to perform because of the proximity of the Rayleigh line. The use of an iodine cell which absorbs the 5145-Å laser line would greatly improve their observation. An experimental Raman setup including such a device across the scattered beam is now in progress.

[1]C. Colvard, R. Merlin, M. V. Klein, and A. C. Gossard, Phys. Rev. Lett. **45**, 298 (1980).

[2]J. Sapriel, J. C. Michel, J. C. Toldedano, R. Vacher, J. Kervarec, and A. Regreny, Phys. Rev. B **28**, 2007 (1983).

[3]D. Kirilov, P. Ho, and G. A. Davis, Appl. Phys. Lett. **48**, 53 (1986).

[4]B. Jusserand and J. Sapriel, Phys. Rev. B **24**, 7194 (1981).

[5]S. M. Rytov, Akust. Zh. **2**, 71 (1956) [Sov. Phys.—Acoust. **2**, 68 (1956)].

[6]B. Jusserand, F. Alexandre, D. Paquet, and G. Leroux, Appl. Phys. Lett. **47**, 301 (1985).

[7]C. Colvard, T. A. Grant, M. V. Klein, R. Merlin, R. Fisher, H. Morkoç, and A. C. Gossard, Phys. Rev. B **31**, 2080 (1985).

[8]H. Bilz and W. Kress, *Phonon Dispersion Relations in Insulators* (Springer-Verlag, Berlin, 1979).

[9]A. K. Sood, J. Menendez, M. Cardona, and K. Ploog, Phys. Rev. Lett. **54**, 2111 (1985).